

# SKA Sensitivity to Sub-GeV Dark Matter Decay: Synchrotron Radio Emissions in White Dwarf Magnetospheres

Kenji Kadota<sup>1,2</sup> and Shota Kisaka<sup>3</sup>

<sup>1</sup>School of Fundamental Physics and Mathematical Sciences, Hangzhou Institute for Advanced Study, University of Chinese Academy of Sciences (HIAS-UCAS), Hangzhou 310024, China

<sup>2</sup>International Centre for Theoretical Physics Asia-Pacific (ICTP-AP), Beijing/Hangzhou, China

<sup>3</sup>Physics Program, Graduate School of Advanced Science and Engineering, Hiroshima University, Higashi-Hiroshima, 739-8526, Japan

We investigate the potential of the Square Kilometre Array (SKA) in detecting synchrotron radiation emitted from the decay of sub-GeV dark matter (dark matter with masses below the GeV scale) in the presence of strong magnetic fields. As a concrete setup, we consider scenarios where the magnetosphere of a magnetic white dwarf overlaps with dense dark matter environments, such as those surrounding a primordial black hole. Our study reveals that the encounters of compact objects such as white dwarfs and black holes offer a promising avenue for upcoming radio telescopes to probe the properties of light dark matter, which has been less explored compared with more conventional heavier (masses above the GeV scale) dark matter.

## I. INTRODUCTION

The nature of the dark matter, such as its mass and interaction, remain elusive despite the compelling supports for its existence from the astrophysical observations. While many conventional dark matter search experiments have targeted weak-scale dark matter (typical mass scale is of order  $\sim 100$  GeV), the lack of observational signals has expanded our interest in exploring a broader range of potential dark matter candidates. The possible dark matter mass can indeed span a wide spectrum, from ultra-light axion-like particles with masses even below  $\mathcal{O}(10^{-20})$  eV to scales surpassing the Planck scale, such as primordial black hole dark matter [1–6].

Our paper focuses on the decay of sub-GeV dark matter (masses below 1 GeV scale), which has not been fully explored in comparison to heavier dark matter [7–19]. Specifically, we are investigating synchrotron radiation signals in dense dark matter environments in the presence of strong magnetic fields. More concretely, we consider the ultra-compact minihalo around a primordial black hole as a dense dark matter environment, and the magnetic white dwarf as the source of a strong magnetic field.

The dark matter can accrete into a black hole to form the ultra compact minihalo and their consequent decay or annihilation from such a large density region has been studied for the detection, for instance, by the gamma-ray, CMB (Cosmic Microwave Background), radio and neutrino telescopes [20–39]. The effects of the dense dark matter environment on gravitational wave signals also have been studied, for instance, through the de-phasing effects of the gravitational waveform by the LISA-like satellite experiments [40–53].

One of reasons why the light (sub-GeV) dark matter is preferable for our signals is that heavier dark matter leads to the peak frequency of synchrotron radiation signals (the peak frequency is proportional to the magnetic field times square of charged particles' Lorentz factor  $\propto B\gamma^2$ ) too big for the SKA [54, 55] sensitive frequency range

(around  $50\text{MHz} - 50\text{GHz}$ ). Another notable difference from the previous works is that we consider the strong magnetic fields from the magnetic white dwarfs. Many previous works studying the synchrotron radiation signals from the dark matter decay and annihilation considered the heavy (mass above GeV scale) dark matter in the presence of the magnetic fields typically of order  $\mathcal{O}(1 - 10)\mu\text{G}$  including those from Galactic center, globular clusters, dwarf galaxies and galaxy clusters [56–62]. For instance Ref. [39] studied synchrotron radiation from the ultra compact minihalos surrounding black holes in the presence of the Galactic magnetic fields. The synchrotron radiation is indeed the dominant radiation for the weak scale dark matter for the magnetic fields of order  $\mathcal{O}(1 - 10)\mu\text{G}$ , which leads to the tight bounds on the abundance of ultra compact minihalos from the currently available radio observation data. For the sub-GeV dark matter mass with such small magnetic fields, due to the smaller energy of final products emitted by the dark matter, the synchrotron radiation power amplitude and peak frequency become too low to be observable by the radio telescopes. See, for instance, Ref. [63] for the scenarios where the inverse Compton scattering, which has a higher peak frequency than that of synchrotron radiation, can instead lead to the radio frequency flux detectable by the SKA for sub-GeV dark matter with order  $\mathcal{O}(1 - 10)\mu\text{G}$  magnetic fields.

In our paper, we focus on the significantly larger magnetic fields of the order  $\mathcal{O}(10^3 - 10^7)\text{G}$  from magnetic white dwarfs. With such large magnetic fields, sub-GeV dark matter can lead to the radio frequency signals within a reach of upcoming SKA radio telescope. In the presence of these intense magnetic fields, the other background photon energy becomes negligible compared with the magnetic field energy, and the synchrotron emission can be the dominant radiation mechanism at radio frequencies. For even higher magnetic fields such as those from the neutron star magnetosphere, however, the peak frequency of the synchrotron radiation can be too high

for the SKA sensitive frequency range in our scenarios. Additionally, the larger volume of the magnetosphere of a white dwarf, from which the signals originate, compared to that of a neutron star, is also advantageous for our scenarios.

Our paper is structured as follows. Section II outlines our formalism to estimate the synchrotron radiation from the dark matter decay, and illustrates the realization of dense dark matter environment surrounding a primordial black hole. Section III presents our findings on the lower bounds of the dark matter decay rate required for detectability by the forthcoming SKA radio telescope.

## II. SETUP

We consider the synchrotron radiation from the relativistic electrons in the presence of strong magnetic fields. As a source of the relativistic electrons, we consider the decaying dark matter. For the strong magnetic fields, we consider the magnetic white dwarfs. In addition, our scenarios assume the dense dark matter environments. We hence also briefly discuss the ultra compact minihalo surrounding a primordial black hole as a concrete realization for large dark matter density.

### A. Synchrotron radiation from dark matter decay

The synchrotron radiation flux density received on the Earth is

$$S_\nu = \frac{1}{D^2} \int_{R_1}^{R_2} dr r^2 j_\nu \quad (1)$$

$D$  is the luminosity distance from the source of the synchrotron radiation to the Earth. The emissivity of the synchrotron radiation source (the energy emitted per unit volume, per unit frequency, per unit time) is

$$j_\nu(\nu, r) = 2 \int_{m_e c^2}^{m_\chi/2} dE \frac{dn_e}{dE}(E) P_\nu(\nu, E, r) \quad (2)$$

We for concreteness consider the magnetic white dwarf and the limits of integration,  $R_1, R_2$ , represent the inner and outer radii of the white dwarf magnetosphere. A factor 2 accounts for the contribution both from electrons and positrons. The power radiated by an electron per unit frequency for synchrotron radiation is given by

$$P_\nu = \frac{\sqrt{3}e^3 B(r) \sin(\alpha)}{m_e c^2} F(x) \quad (3)$$

where  $\alpha$  is the pitch angle (the angle between the velocity vector of the electron and the magnetic field).  $F(x)$  is the synchrotron function (the low frequency part is well approximated by the power law of  $1/3$  and decays exponentially well above the critical frequency)

$$F(x) = x \int_x^\infty K_{5/3}(\xi) d\xi \quad (4)$$

$K_{5/3}$  is the modified Bessel function of the second kind of order  $5/3$ , and  $x = \nu/\nu_c$ , where  $\nu_c = 3eB\gamma^2 \sin(\alpha)/(4\pi m_e c)$  is the critical frequency. We assume the simple dipole profile  $B(r) \propto r^{-3}$  for the white dwarf magnetic field. The electron energy spectrum  $\frac{dn_e}{dE}$  (the electron number density per unit energy) arising from the dark matter decay can be estimated as

$$\frac{dn_e}{dE} \approx n_\chi \Gamma_\chi \times \min[t_{cool}, t_{ad}] \times \frac{dN_e}{dE} \quad (5)$$

where  $n_\chi, \Gamma_\chi$  are respectively the dark matter number density and decay rate.  $dN_e/dE$  represents the electron energy distribution from each dark matter decay for a given final state channel. We assume for illustration the dark matter decays dominantly into electron positron pair final states  $\chi \rightarrow e^+ e^-$ . Two timescales  $t_{cool}, t_{ad}$  are the cooling timescale and the advection timescale. The cooling timescale of synchrotron radiation can be estimated by

$$t_{cool} \sim \frac{\gamma m_e c^2 \sin \alpha}{P_{syn}} \quad (6)$$

$$\sim 4 \times 10^{-5} \left( \frac{10^5 G}{B(r)} \right)^2 \left( \frac{10^2}{\gamma} \right) \left( \frac{1}{\sin \alpha} \right) [s] \quad (7)$$

$\gamma$  is the Lorentz factor of a radiating charged particle and  $P_{syn}$  is the total power (integrated over all frequency) of the synchrotron radiation for each particle

$$P_{syn} = \frac{2e^4 B(r)^2 \gamma^2 \beta^2 \sin^2 \alpha}{3m_e^2 c^3} \quad (8)$$

The advection timescale at the emission region  $r$  can be estimated by

$$t_{ad} \sim \frac{r}{c} \sim 0.2 \left( \frac{r}{0.1 R_\odot} \right) [s] \quad (9)$$

When we integrate over the white dwarf magnetosphere, the magnetic field is bigger for a smaller radius while there is a bigger volume contribution for a bigger radius. The relevant timescale, the minimum of  $t_{cool}$  and  $t_{ad}$ , becomes biggest at a radius where  $t_{cool} \approx t_{ad}$ .

We consider the magnetic white dwarf as the source of the strong magnetic field. The magnetic white dwarfs (MWDs) are characterized by the strong magnetic fields and they can make up of order  $\mathcal{O}(10)\%$  of the white dwarf population [64–66]. The magnetic fields of MWDs can typically range from  $10^3 G$  to  $10^9 G$ , and some of closest known MWDs are within 20 parsecs of the Earth. In our quantitative discussions in Section III, we choose the distance to the white dwarf  $D = 100 pc$ , its radius  $R_1 = 0.01 R_\odot$ , the size of the magnetosphere  $R_2 = 10 \times R_1$ , the pitch angle  $\sin \alpha = 1$  as the fiducial values for illustration. We will demonstrate, in Section III, that a magnetic field of around  $10^6 G$  on the surface of a white dwarf represents an optimal value for our signal estimates. Larger magnetic fields result in signal peak frequencies falling

outside the SKA sensitivity window, despite an increase in signal amplitude with stronger magnetic fields<sup>1</sup>.

### B. Dense dark matter environment around a primordial black hole

The signals of indirect dark matter search can be enhanced in the presence of the dense dark matter environment. As a concrete example to realize such a high density dark matter region, we illustrate the ultra-compact minihalo surrounding a primordial black hole. We adopt the analytical expression of Refs.[27–29, 67, 68] which is given by (for brevity, we use the convention  $c = 1$  in the following discussions unless stated otherwise)<sup>2</sup>

$$\rho_\chi(x) = \begin{cases} \rho_{kd} \left(\frac{r_c}{r}\right)^{3/4} & \text{for } r \leq r_c \\ \frac{\rho_{eq}}{2} \left(\frac{M}{M_\odot}\right)^{3/2} \left(\frac{\hat{r}}{r}\right)^{3/2} & \text{for } r_c < r \leq r_k \\ \frac{\rho_{eq}}{2} \left(\frac{M}{M_\odot}\right)^{3/4} \left(\frac{\bar{r}}{r}\right)^{9/4} & \text{for } r > r_k \end{cases} \quad (10)$$

where

$$\hat{r} \equiv GM_\odot \frac{t_{eq} m_\chi}{t_{kd} T_{kd}}, \bar{r} \equiv (2GM_\odot t_{eq}^2)^{1/3} \quad (11)$$

The transition radii are given by

$$r_c \sim \frac{r_{sch}}{2} \left(\frac{m_\chi}{T_{kd}}\right), r_k \sim 4 \frac{t_{kd}^2}{r_{sch}} \left(\frac{T_{kd}}{m_\chi}\right)^2 \quad (12)$$

where  $r_{sch} = 2GM$  is the Schwarzschild radius for a given black hole mass  $M$ .  $\rho_{eq}, t_{eq}$  are respectively the density of the Universe and the time at the matter-radiation equality epoch.  $\rho_{kd}, t_{kd}$  are those at the dark matter kinetic decoupling. The epoch when the dark matter kinetically decouples from the cosmic plasma affects the velocity of dark matter, and it can influence the dark matter profile because the dark matter kinetic energy can play an important role in how it is trapped by a black hole's gravitational field. The dark matter kinetic decoupling temperature  $T_{kd}$  is given by<sup>3</sup>

$$T_{kd} = \frac{m_\chi^{5/4}}{\Gamma[3/4]} \left(\frac{\alpha}{M_{pl}}\right)^{1/4} \quad (13)$$

<sup>1</sup> We also mention that the magnetosphere of a neutron star could be an alternative possibility for our setups. We however found that the magnetosphere of a white dwarf is more suitable to our scenarios than that of a neutron star, due to its relatively weaker magnetic field (ensuring signal frequencies within the SKA's sensitivity range) and its larger volume (allowing for greater spatial overlap with dark matter).

<sup>2</sup> For concreteness, we assume a primordial black hole rather than an astrophysically sourced black hole. The purpose of this section is simply to illustrate an example of a large dark matter density. The discussions on radio emissions in subsequent sections, while focused on this context, can also qualitatively apply to other environments with dense dark matter.

<sup>3</sup> The exact nature of the kinetic decoupling can be heavily model-dependent. We refer the readers to, for instance, Refs. [69–76] for more detailed physics and the phenomenology of dark matter kinetic decoupling.

and the corresponding kinetic decoupling time is obtained from the Friedmann equation

$$t_{kd} = \frac{m_{pl}}{2\alpha T_{kd}^2} \quad (14)$$

with  $\alpha = (16\pi^3 g_{kd}/45)^{1/2}$ . For concreteness, we choose the relativistic degrees of freedom at the kinetic decoupling  $g_{kd} = 61.75$  [26, 27, 76].  $\Gamma$  is the gamma function. We refer the readers to Refs.[27–29, 67, 68, 77, 78] for more detailed discussions on the dark matter profile.

The profiles are illustrated in Fig. 1. The curve is truncated at the Schwarzschild radius. Such a profile can be

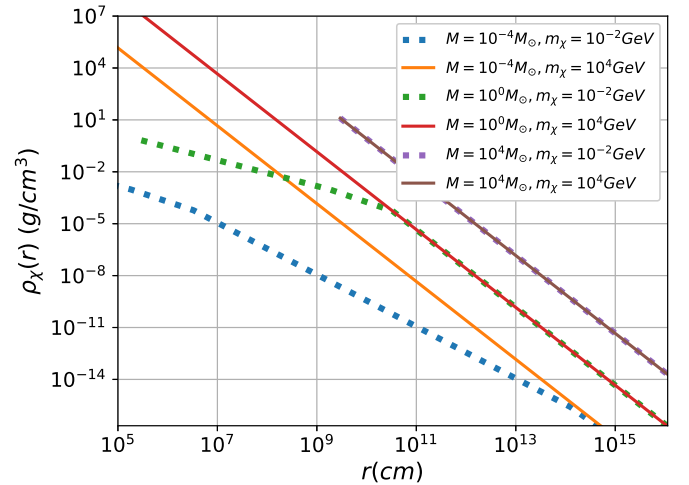


FIG. 1: The enhanced dark matter density around a primordial black hole for different black hole masses ( $M = 10^{-4}, 1, 10^4 M_\odot$ ) and dark matter masses ( $m_\chi = 10^{-2} \text{ GeV}, 10^4 \text{ GeV}$ ). The curve is truncated at Schwarzschild radius. Two curves for  $M = 10^4 M_\odot$  with  $m_\chi = 10^{-2}$  and  $m_\chi = 10^4 \text{ GeV}$  are indistinguishable.

obtained analytically assuming the adiabatic growth of a halo and it has also been verified numerically [24, 26, 79]<sup>4</sup>. For the radius below  $r_k$  (which characterizes the scale inside which the dark matter particle kinetic energy is bigger than its potential energy under the influence of the gravitational field of the central object (such as a black hole)), the slope becomes milder. The halo profile for

<sup>4</sup> The power for the spike profile  $\rho(r) \propto r^{-\gamma_{sp}}$  for a given initial profile  $\rho_{ini} \propto r^{-\gamma_{ini}}$  can be analytically derived as  $\gamma_{sp} = (9 - 2\gamma_{ini})/(4 - \gamma_{ini})$ . For instance,  $\gamma_{sp} = 9/4$  for the spike profile around a primordial black hole with the initial background  $\gamma_{ini} = 0$  deep in the radiation dominated epoch, and  $\gamma_{sp} = 7/3$  if the halo growth starts from the cuspy NFW profile  $\gamma_{ini} = 1$ . A steeper slope can lead to a bigger density and some literature discusses even a value up to  $\gamma_{sp} \sim 2.75$  [24, 80–83]. Our qualitative discussions and conclusions are not affected by those choices of parameters and we show the density profile for  $\gamma_{sp} = 9/4$  in Fig. 1 to illustrate a possible realization of a large dark matter density.

such an inner region can be obtained analytically by requiring the phase space conservation assuming Maxwell-Boltzmann distribution for the dark matter velocity [27–29, 67, 68].

Having illustrated how big the dark matter density can be around a primordial black hole, which even could reach the values be as big as  $\mathcal{O}(1)g/cm^3$ , we simply adopt the value  $\rho_\chi = 1g/cm^3$  as the fiducial value for quantitative discussions in Section III. Readers can straightforwardly re-scale our calculation results for a different value because our synchrotron radiation signal (Eq. (1)) scales linearly with  $\rho_\chi$ . We mention that the dynamics of white dwarf motion in a high dark matter density environment, especially near a black hole, can be complex. Our objective is to explore the potential effects of such an environment, serving as a proof of concept for the parameters we have adopted. Our preliminary investigation aims to understand the implications of a white dwarf encountering a region rich in dark matter. In our present analysis, we disregard variations in dark matter density, since the synchrotron radiation is promptly emitted in strong magnetic fields. This suffices for our goal of demonstrating the potential significance of our scenarios for the future radio observations.

### III. RESULTS

We compare the possible signals in our scenarios with the forthcoming SKA sensitivity [54, 55]. The SKA sensitivity is estimated by the radiometer equation

$$S_{min} = \frac{2k_b T_{sys}}{A_{eff} \eta_s \sqrt{\eta_{pol} t_{obs} \Delta B}} \quad (15)$$

$k_b$  is the Boltzmann constant,  $\eta_{pol}$  is the number of polarization states,  $t_{obs}$  is the integrated observation time.  $A_{eff}$  is the effective collecting area of the telescope and  $T_{sys}$  is the system temperature consisting of the sum of sky/instrumental noises of the system. Note their ratio  $A_{eff}/T_{sys}$ , so-called the natural sensitivity, is frequency dependent and the values are adopted from Ref. [55].  $\eta_s$  is the system efficiency and  $\Delta B$  is the bandwidth. We use  $\eta_s = 0.9$ ,  $\eta_{pol} = 2$  and adopt the band width which is frequency dependent as 0.3 times the frequency  $\Delta B = 0.3\nu$  [55]. The anticipated sensitivity of the upcoming SKA is expected to cover the frequency range  $50MHz \sim 50GHz$  (combining SKA-Low (covering the lower frequency bands) and SKA-Mid (covering the mid-range frequencies)).

Fig. 2 shows the energy spectrum distribution  $\nu S_\nu$  of our estimated signals (flux density multiplied by frequency, and the integral  $\nu S_\nu$  over  $\ln \nu$  represents the total energy flux) for different dark matter masses (top panel) and for different magnetic field amplitudes (bottom), along with the SKA sensitivities for  $t_{obs} = 100$  and 1000 hours of observations.

Fig. 2 also illustrates the cutoff at low frequencies, which is a characteristic feature of synchrotron radiation.

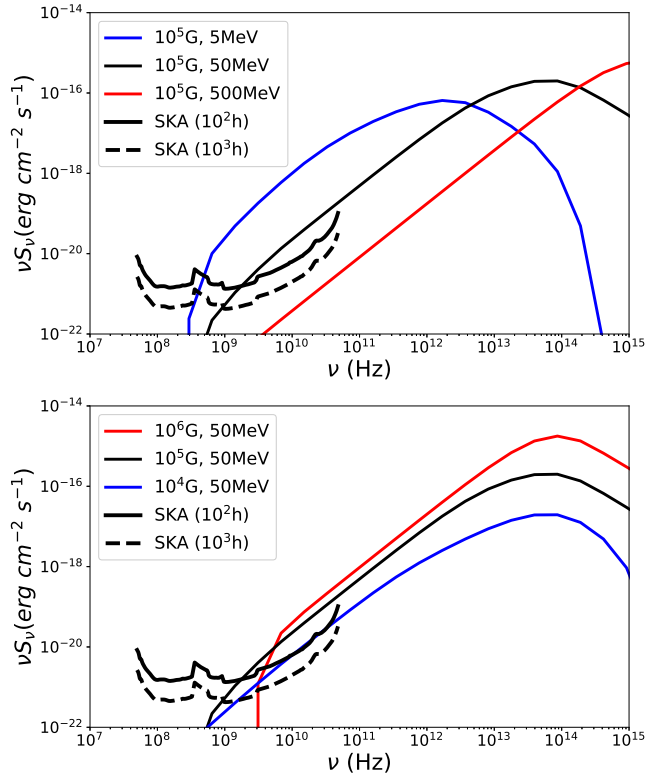


FIG. 2: The energy spectrum distribution  $\nu S_\nu$  for the synchrotron radiation as a function of the frequency. The SKA sensitivity assuming 100 and 1000 hours of observations are shown for reference. The magnetic white dwarf is assumed to be 100 pc away from the Earth. We assume that the magnetic field follows the dipole profile  $B(r) = B_0(r/r_0)^{-3}$  and the magnetosphere spans from  $r_0 = 0.01R_\odot$  to  $10r_0$ . The dark matter decay rate  $\Gamma_\chi = 10^{-25}[s^{-1}]$  and the density  $\rho_\chi = 1[g/cm^3]$  are used. The top panel displays the cases for dark matter masses  $m_\chi = 5\text{MeV}, 50\text{MeV}, 500\text{MeV}$  with a magnetic field coefficient  $B_0 = 10^5\text{G}$ . The bottom panel illustrates various magnetic field amplitudes with  $B_0 = 10^6, 10^5, 10^4\text{G}$  for a constant dark matter mass of  $m_\chi = 50\text{MeV}$ .

The synchrotron radiation becomes negligible at frequencies below the Larmor frequency  $\nu_L = eB(r)/2\pi m_e$  [84, 85]. For illustration purposes, we applied a cutoff to the synchrotron radiation power  $P_\nu(\nu, r)$  so that the radiation vanishes when the frequency is below the Larmor frequency  $\nu \leq \nu_L$  in our integrating the radiation contributions over the white dwarf magnetosphere.

The top panel of Fig. 2 displays the energy spectrum distribution across different dark matter masses, while the bottom panel illustrates variations due to changing magnetic fields. We observe a general trend of increasing peak frequency and emitted total power (represented by the area under the curve) in the figure with larger dark matter masses and magnetic field strengths. The shift

in peak frequency however is not simply proportional to  $\gamma^2 B_0$ , and likewise, the total emitted power dependence on  $\gamma, B_0$  is not trivial either. This is attributed to the integration of the synchrotron radiation contribution over the position dependent magnetic field profile within the white dwarf magnetosphere. For a larger radius, the magnetic field becomes small even though there is a bigger volume factor. In fact, in some regions of the magnetosphere, particularly for smaller values of  $\gamma$  and  $B(r)$ , synchrotron radiation cooling is less efficient and the advection timescale can become comparable to, or shorter than, the radiation cooling timescale. The resultant synchrotron radiation energy spectrum hence can possess non-trivial dependence on  $\gamma, B$ .

Having obtained the radiation spectrum, we can now put the bounds on the dark matter decay rate  $\Gamma_\chi$ . We conservatively obtain the bounds on  $\Gamma_\chi$  by ensuring that the synchrotron radiation flux does not exceed the SKA threshold across the entire frequency the SKA is sensitive to. It is around 50 MHz to 50 GHz as illustrated in our figures, and we assume 100 hours of SKA observation in deriving the bounds. Fig. 3 shows the resultant lower bounds on  $\Gamma_\chi$  above which our synchrotron radiation signals can be detectable by the SKA. The behavior of the curves for different magnetic fields are caused by the change of the peak frequency and the change of the synchrotron radiation power amplitude.  $B_0 = 10^7 \text{G}$  has a peak frequency well above the SKA sensitive frequencies. Hence the lower magnetic field  $B_0 = 10^6 \text{G}$  with a lower peak frequency can give tighter bounds even though the radiation power is smaller due to the smaller magnetic field (the total synchrotron radiation power is proportional to  $B^2 \gamma^2$ ). For even lower magnetic fields with  $B_0 \lesssim 10^5 \text{G}$ , the synchrotron radiation power reduction causes the weaker bounds on  $\Gamma_\chi$ . Besides the requirement for the dark matter to have the life time longer than the age of the Universe  $\Gamma_\chi^{-1} \gtrsim 4 \times 10^{17} [\text{s}]$ , there are much tighter bounds from other astrophysical observations. For the sub-GeV dark matter, the CMB and Voyager give among the tightest bounds and the upper bounds from the Planck CMB and Voyager data are plotted in Fig. 3 for reference [86–89]. Dark matter decays can inject energy into the cosmic plasma, altering the reionization history and affecting the CMB data. The Voyager data can put bounds on the dark matter from the cosmic ray measurements in the interstellar medium outside the influence of the solar wind<sup>5</sup>. Our study demonstrates that our scenarios involving the white dwarf and

black hole can potentially lead to the signals observable by the SKA even with a small enough dark matter decay rate satisfying other stringent bounds. We also note that there are many magnetic white dwarfs closer than 100 pc away [64, 92], and our signals may well be bigger than those in this figure using the fiducial value of 100 pc (the readers can straightforwardly scale the signals which are inversely proportional to the luminosity distance squared).

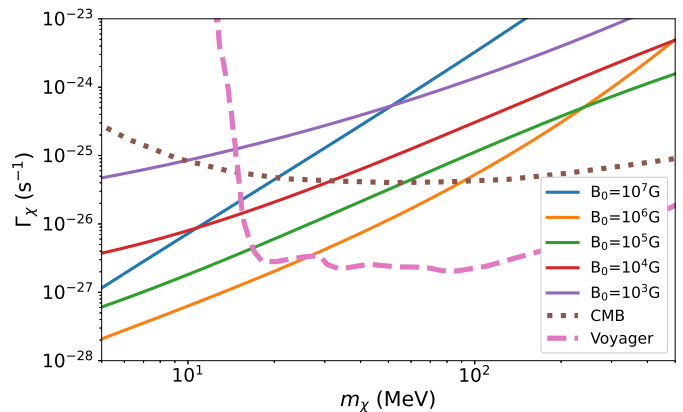


FIG. 3: The lower bounds on the dark matter decay rate  $\Gamma_\chi$  to be detectable by the SKA assuming 100 hours of observation. The dipole magnetic field profile  $B(r) = B_0(r/r_0)^{-3}$  is assumed and the magnetosphere spans from  $r_0 = 0.01R_\odot$  to  $10r_0$ . The bounds for  $B_0 = 10^3 - 10^7 \text{G}$  are shown. The constant dark matter density  $\rho_\chi = 1 \text{g/cm}^3$  is assumed. The upper bounds from the CMB and Voyager data are also plotted for reference.

Before concluding our discussions, let us also briefly discuss the prospects of the synchrotron radiation for our scenarios at the frequencies higher than the radio range relevant for the SKA. For illustration, Fig. 4 shows the energy spectrum covering X-ray and gamma-ray frequencies in addition to the radio range. For the large dark matter mass above GeV scale, there currently exist tight upper bounds on dark matter decay rate  $\Gamma_\chi$  from the X-ray and gamma-ray indirect dark matter search [87]. For instance, for the sub-GeV dark matter, the bounds are of order  $\Gamma_\chi^{-1} \gtrsim 10^{25} \text{sec}$ , and, for the mass above 1 GeV, the bounds are of order  $10^{27} \sim 10^{28} \text{sec}$ . We accordingly adopt the fiducial values of  $\Gamma = 10^{-25} [\text{s}^{-1}]$  for  $m_\chi < 1 \text{GeV}$ ,  $10^{-27} [\text{s}^{-1}]$  for  $1 \text{GeV} \leq m_\chi < 1 \text{TeV}$  and  $10^{-28} [\text{s}^{-1}]$  for  $m_\chi \geq 1 \text{TeV}$  in calculating our synchrotron radiation signals in Fig. 4 [11, 86, 93]. Fig. 4 also shows the sensitivity of the currently available observation data for the X-ray and gamma-ray observations (Chandra, NuSTAR and Fermi assuming 100 hours of observations) [56, 94–96]. We can see that experiments targeting frequencies higher than the radio range exhibit less competitive sensitivity compared to the superior sensitivity expected from the

<sup>5</sup> The cosmic ray electrons/positrons are usually shielded by the solar magnetic fields for the earth-bound detectors (so-called solar modulation effects), but not for the Voyager which crossed the heliopause. Such Voyager’s unique data sets were compared with a simulation of the expected cosmic-ray electron and positron fluxes originating from dark matter decay to obtain the novel constraints on the dark matter properties [89–91]. The bounds shown in our figure are from the diffuse DM distributions, which are also applicable to our study.

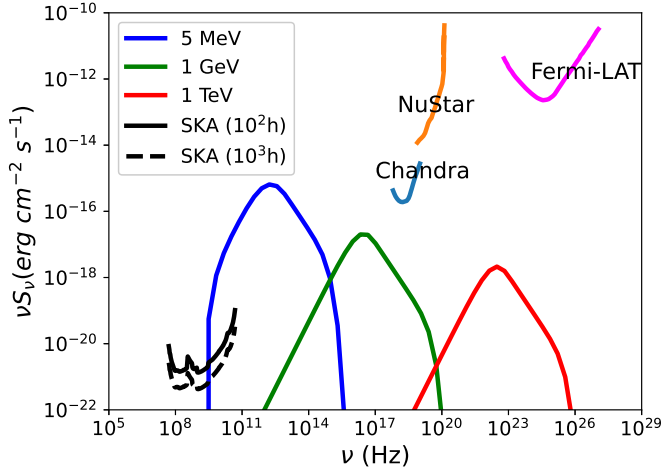


FIG. 4: The energy spectrum distribution  $\nu S_\nu$  for the synchrotron radiation as a function of the frequency.

The magnetic white dwarf is assumed to be 100 pc away and the dark matter density  $\rho_\chi = 1\text{g/cm}^3$  is assumed. The magnetic field follows the dipole profile

$$B(r) = B_0(r/r_0)^{-3} \text{ with } B_0 = 10^6\text{G and the}$$

magnetosphere region is from  $r_0 = 0.01R_\odot$  to  $10r_0$ . The dark matter masses for  $m_\chi = 5\text{MeV}, 1\text{GeV}, 1\text{TeV}$  are shown. The sensitivity of different experiments are also shown covering the radio (SKA assuming 100 and 1000 hours of observations), X-ray (Chandra, NuSTAR) and gamma-ray (Fermi-LAT) frequencies. 100 hours of observations are assumed for Chandra, NuSTAR and Fermi-LAT sensitivity curves.

SKA. This is partly due to the large effective area that radio telescopes, such as the SKA, can boast.

We investigated potential SKA probes of synchrotron radiation resulting from sub-GeV dark matter decay in the presence of strong magnetic fields. We specifically examined scenarios where dark matter environments around a primordial black hole overlap with the magnetosphere of a magnetic white dwarf. Our estimates suggest that the encounters of compact objects, such as white dwarfs and black holes, could present compelling

targets for upcoming radio telescopes to clarify the nature of dark matter. While our scenarios primarily require the singular encounters with unbound orbits, the possibly rarer yet intriguing scenarios of binary formation would also warrant further exploration. The black hole-white dwarf binary system has been less explored in the literature compared with black hole-black hole and black hole-neutron star binaries. The black hole-white dwarf binaries can be of great interest for the targets of multi-messenger objects. The black hole-white dwarf binaries have been also studied for the gravitational wave signals. For example, the detection of  $\mathcal{O}(10)$  PBH-White dwarf merger events is feasible for  $M_{PBH} \sim 10^5 M_\odot$  by the DECIGO-like space-borne gravitational wave interferometer within three years at distances up to  $\sim 1$  Gpc scale [97]. We however note that these estimations of event rates significantly depend on the assumptions of underlying models, such as the mass functions of compact objects. For more detailed discussions on calculation methodologies and model dependencies for the estimation of the compact object encountering rate, we direct readers to the pertinent literature [97–106].

The detailed estimation for the black hole-white dwarf encountering rates relevant for our scenarios are left for future work. The potential X-ray, gamma-ray and gravitational wave signals have been studied for the white dwarf-black hole binaries, but radio signals have received little attention [98, 99, 102–108]. More detailed analyses of our scenarios, including tidal effects and the possible binary formation, will be addressed in future numerical studies.

## ACKNOWLEDGMENT

We thank N. Kitajima and K. Toma for the useful discussions. KK thanks the CTPU at IBS for their hospitality during the completion of this work. This work was supported by Center of Quantum Cosmo Theoretical Physics (NSFC grant No. 12347103), KAKENHI Grants No. JP21H01078, No. JP22H01267, and No. JP22K03681.

- 
- [1] G. Jungman, M. Kamionkowski, and K. Griest, Super-symmetric dark matter, *Phys. Rept.* **267**, 195 (1996), arXiv:hep-ph/9506380.
- [2] G. Arcadi, M. Dutra, P. Ghosh, M. Lindner, Y. Mambrini, M. Pierre, S. Profumo, and F. S. Queiroz, The waning of the WIMP? A review of models, searches, and constraints, *Eur. Phys. J. C* **78**, 203 (2018), arXiv:1703.07364 [hep-ph].
- [3] K. K. Boddy et al., Snowmass2021 theory frontier white paper: Astrophysical and cosmological probes of dark matter, *JHEAp* **35**, 112 (2022), arXiv:2203.06380 [hep-ph].
- [4] A. S. Chou et al., Snowmass Cosmic Frontier Report, in *2022 Snowmass Summer Study* (2022) arXiv:2211.09978 [hep-ex].
- [5] B. Carr and F. Kuhnel, Primordial Black Holes as Dark Matter: Recent Developments, (2020), arXiv:2006.02838 [astro-ph.CO].
- [6] F. Chadha-Day, J. Ellis, and D. J. E. Marsh, Axion dark matter: What is it and why now?, *Sci. Adv.* **8**, abj3618 (2022), arXiv:2105.01406 [hep-ph].

- [7] S. Knapen, T. Lin, and K. M. Zurek, Light Dark Matter: Models and Constraints, *Phys. Rev. D* **96**, 115021 (2017), arXiv:1709.07882 [hep-ph].
- [8] M. Battaglieri et al., US Cosmic Visions: New Ideas in Dark Matter 2017: Community Report, in *U.S. Cosmic Visions: New Ideas in Dark Matter* (2017) arXiv:1707.04591 [hep-ph].
- [9] K. Bondarenko, A. Boyarsky, T. Bringmann, M. Hufnagel, K. Schmidt-Hoberg, and A. Sokolenko, Direct detection and complementary constraints for sub-GeV dark matter, *JHEP* **03**, 118, arXiv:1909.08632 [hep-ph].
- [10] A. Coogan, L. Morrison, and S. Profumo, Hazma: A Python Toolkit for Studying Indirect Detection of Sub-GeV Dark Matter, *JCAP* **01**, 056, arXiv:1907.11846 [hep-ph].
- [11] R. Essig, E. Kuflik, S. D. McDermott, T. Volansky, and K. M. Zurek, Constraining Light Dark Matter with Diffuse X-Ray and Gamma-Ray Observations, *JHEP* **11**, 193, arXiv:1309.4091 [hep-ph].
- [12] M. Cirelli, N. Fornengo, B. J. Kavanagh, and E. Pinetti, Integral X-ray constraints on sub-GeV Dark Matter, *Phys. Rev. D* **103**, 063022 (2021), arXiv:2007.11493 [hep-ph].
- [13] D. Choudhury and D. Sachdeva, Model independent analysis of MeV scale dark matter: Cosmological constraints, *Phys. Rev. D* **100**, 035007 (2019), arXiv:1903.06049 [hep-ph].
- [14] D. Hooper, M. Kaplinghat, L. E. Strigari, and K. M. Zurek, MeV Dark Matter and Small Scale Structure, *Phys. Rev. D* **76**, 103515 (2007), arXiv:0704.2558 [astro-ph].
- [15] H. Tashiro, K. Kadota, and J. Silk, Effects of dark matter-baryon scattering on redshifted 21 cm signals, *Phys. Rev. D* **90**, 083522 (2014), arXiv:1408.2571 [astro-ph.CO].
- [16] W. L. Xu, C. Dvorkin, and A. Chael, Probing sub-GeV Dark Matter-Baryon Scattering with Cosmological Observables, *Phys. Rev. D* **97**, 103530 (2018), arXiv:1802.06788 [astro-ph.CO].
- [17] J. Ooba, H. Tashiro, and K. Kadota, Cosmological constraints on the velocity-dependent baryon-dark matter coupling, *JCAP* **09**, 020, arXiv:1902.00826 [astro-ph.CO].
- [18] C. Boehm, T. A. Ensslin, and J. Silk, Can Annihilating dark matter be lighter than a few GeVs?, *J. Phys. G* **30**, 279 (2004), arXiv:astro-ph/0208458.
- [19] M. Cirelli, N. Fornengo, J. Koechler, E. Pinetti, and B. M. Roach, Putting all the X in one basket: Updated X-ray constraints on sub-GeV Dark Matter, *JCAP* **07**, 026, arXiv:2303.08854 [hep-ph].
- [20] B. Carr, S. Clesse, J. Garcia-Bellido, M. Hawkins, and F. Kuhnel, Observational Evidence for Primordial Black Holes: A Positivist Perspective, (2023), arXiv:2306.03903 [astro-ph.CO].
- [21] K. Freese, I. Galstyan, P. Sandick, and P. Stengel, Neutrino point source searches for dark matter spikes, *JCAP* **08**, 065, arXiv:2202.01126 [astro-ph.CO].
- [22] F. Kuhnel and T. Ohlsson, Decaying Dark Matter in Halos of Primordial Black Holes, *Eur. Phys. J. C* **79**, 687 (2019), arXiv:1811.05810 [astro-ph.CO].
- [23] P. Scott and S. Sivertsson, Gamma-Rays from Ultracompact Primordial Dark Matter Minihalos, *Phys. Rev. Lett.* **103**, 211301 (2009), [Erratum: *Phys. Rev. Lett.* **105**, 119902 (2010)], arXiv:0908.4082 [astro-ph.CO].
- [24] P. Gondolo and J. Silk, Dark matter annihilation at the galactic center, *Phys. Rev. Lett.* **83**, 1719 (1999), arXiv:astro-ph/9906391.
- [25] B. C. Lacki and J. F. Beacom, Primordial Black Holes as Dark Matter: Almost All or Almost Nothing, *Astrophys. J. Lett.* **720**, L67 (2010), arXiv:1003.3466 [astro-ph.CO].
- [26] J. Adamek, C. T. Byrnes, M. Gosenca, and S. Hotchkiss, WIMPs and stellar-mass primordial black holes are incompatible, *Phys. Rev. D* **100**, 023506 (2019), arXiv:1901.08528 [astro-ph.CO].
- [27] S. M. Boucenna, F. Kuhnel, T. Ohlsson, and L. Visinelli, Novel Constraints on Mixed Dark-Matter Scenarios of Primordial Black Holes and WIMPs, *JCAP* **07**, 003, arXiv:1712.06383 [hep-ph].
- [28] Y. Eroshenko, Dark matter density spikes around primordial black holes, *Astron. Lett.* **42**, 347 (2016), arXiv:1607.00612 [astro-ph.HE].
- [29] B. Carr, F. Kuhnel, and L. Visinelli, Black holes and WIMPs: all or nothing or something else, *Mon. Not. Roy. Astron. Soc.* **506**, 3648 (2021), arXiv:2011.01930 [astro-ph.CO].
- [30] R.-G. Cai, X.-Y. Yang, and Y.-F. Zhou, Constraints on mixed dark matter model of particles and primordial black holes from the Galactic 511 keV line, (2020), arXiv:2007.11804 [astro-ph.CO].
- [31] M. S. Delos, A. L. Erickcek, A. P. Bailey, and M. A. Alvarez, Density profiles of ultracompact minihalos: Implications for constraining the primordial power spectrum, *Phys. Rev. D* **98**, 063527 (2018), arXiv:1806.07389 [astro-ph.CO].
- [32] K. Kohri, T. Nakama, and T. Suyama, Testing scenarios of primordial black holes being the seeds of supermassive black holes by ultracompact minihalos and CMB  $\mu$ -distortions, *Phys. Rev. D* **90**, 083514 (2014), arXiv:1405.5999 [astro-ph.CO].
- [33] G. Bertone, A. M. Coogan, D. Gaggero, B. J. Kavanagh, and C. Weniger, Primordial Black Holes as Silver Bullets for New Physics at the Weak Scale, *Phys. Rev. D* **100**, 123013 (2019), arXiv:1905.01238 [hep-ph].
- [34] S. Ando and K. Ishiwata, Constraints on decaying dark matter from the extragalactic gamma-ray background, *JCAP* **05**, 024, arXiv:1502.02007 [astro-ph.CO].
- [35] M. P. Hertzberg, S. Nurmi, E. D. Schiappacasse, and T. T. Yanagida, Shining Primordial Black Holes, (2020), arXiv:2011.05922 [hep-ph].
- [36] Y. Yang, The abundance of primordial black holes from the global 21cm signal and extragalactic gamma-ray background, *Eur. Phys. J. Plus* **135**, 690 (2020), arXiv:2008.11859 [astro-ph.CO].
- [37] D. Zhang, Impact of Primordial Ultracompact Minihaloes on the Intergalactic Medium and First Structure Formation, *Mon. Not. Roy. Astron. Soc.* **418**, 1850 (2011), arXiv:1011.1935 [astro-ph.CO].
- [38] H. Tashiro and K. Kadota, Constraining Mixed Dark-Matter Scenarios of WIMPs and Primordial Black Holes from CMB and 21-cm observations, *Phys. Rev. D* **103**, 123532 (2021), arXiv:2104.09738 [astro-ph.CO].

- [39] K. Kadota and H. Tashiro, Radio bounds on the mixed dark matter scenarios of primordial black holes and WIMPs, *JCAP* **08** (08), 004, arXiv:2204.13273 [hep-ph].
- [40] K. Eda, Y. Itoh, S. Kuroyanagi, and J. Silk, New Probe of Dark-Matter Properties: Gravitational Waves from an Intermediate-Mass Black Hole Embedded in a Dark-Matter Minispike, *Phys. Rev. Lett.* **110**, 221101 (2013), arXiv:1301.5971 [gr-qc].
- [41] K. Eda, Y. Itoh, S. Kuroyanagi, and J. Silk, Gravitational waves as a probe of dark matter minispikes, *Phys. Rev. D* **91**, 044045 (2015), arXiv:1408.3534 [gr-qc].
- [42] K. Kadota and J. Silk, Boosting small-scale structure via primordial black holes and implications for sub-GeV dark matter annihilation, *Phys. Rev. D* **103**, 043530 (2021), arXiv:2012.03698 [astro-ph.CO].
- [43] X.-J. Yue and W.-B. Han, Gravitational waves with dark matter minispikes: the combined effect, *Phys. Rev. D* **97**, 064003 (2018), arXiv:1711.09706 [gr-qc].
- [44] C. F. B. Macedo, P. Pani, V. Cardoso, and L. C. B. Crispino, Into the lair: gravitational-wave signatures of dark matter, *Astrophys. J.* **774**, 48 (2013), arXiv:1302.2646 [gr-qc].
- [45] E. Barausse, V. Cardoso, and P. Pani, Can environmental effects spoil precision gravitational-wave astrophysics?, *Phys. Rev. D* **89**, 104059 (2014), arXiv:1404.7149 [gr-qc].
- [46] G. Bertone *et al.*, Gravitational wave probes of dark matter: challenges and opportunities, *SciPost Phys. Core* **3**, 007 (2020), arXiv:1907.10610 [astro-ph.CO].
- [47] P. S. Cole, G. Bertone, A. Coogan, D. Gaggero, T. Karydas, B. J. Kavanagh, T. F. M. Spieksma, and G. M. Tomaselli, Disks, spikes, and clouds: distinguishing environmental effects on BBH gravitational waveforms, (2022), arXiv:2211.01362 [gr-qc].
- [48] B. J. Kavanagh, D. A. Nichols, G. Bertone, and D. Gaggero, Detecting dark matter around black holes with gravitational waves: Effects of dark-matter dynamics on the gravitational waveform, *Phys. Rev. D* **102**, 083006 (2020), arXiv:2002.12811 [gr-qc].
- [49] V. Cardoso and A. Maselli, Constraints on the astrophysical environment of binaries with gravitational-wave observations, *Astron. Astrophys.* **644**, A147 (2020), arXiv:1909.05870 [astro-ph.HE].
- [50] O. A. Hannuksela, K. C. Y. Ng, and T. G. F. Li, Extreme dark matter tests with extreme mass ratio inspirals, *Phys. Rev. D* **102**, 103022 (2020), arXiv:1906.11845 [astro-ph.CO].
- [51] A. Coogan, G. Bertone, D. Gaggero, B. J. Kavanagh, and D. A. Nichols, Measuring the dark matter environments of black hole binaries with gravitational waves, (2021), arXiv:2108.04154 [gr-qc].
- [52] H. Kim, A. Lenoci, I. Stomberg, and X. Xue, Adiabatically compressed wave dark matter halo and intermediate-mass-ratio inspirals, *Phys. Rev. D* **107**, 083005 (2023), arXiv:2212.07528 [astro-ph.GA].
- [53] K. Kadota, J. H. Kim, P. Ko, and X.-Y. Yang, Gravitational Wave Probes on Self-Interacting Dark Matter Surrounding an Intermediate Mass Black Hole, (2023), arXiv:2306.10828 [hep-ph].
- [54] ska webpage:, <https://www.skao.int/>.
- [55] R. Braun, A. Bonaldi, T. Bourke, E. Keane, and J. Wagg, Anticipated Performance of the Square Kilometre Array – Phase 1 (SKA1), arXiv e-prints , arXiv:1912.12699 (2019).
- [56] J. A. R. Cembranos, A. De La Cruz-Dombriz, V. Gammaldi, and M. Méndez-Isla, SKA-Phase 1 sensitivity to synchrotron radio emission from multi-TeV Dark Matter candidates, *Phys. Dark Univ.* **27**, 100448 (2020), arXiv:1905.11154 [hep-ph].
- [57] S. Colafrancesco, M. Regis, P. Marchegiani, G. Beck, R. Beck, H. Zechlin, A. Lobanov, and D. Horns, Probing the nature of Dark Matter with the SKA, *PoS AASKA14*, 100 (2015), arXiv:1502.03738 [astro-ph.HE].
- [58] Z. Chen, Y.-L. S. Tsai, and Q. Yuan, Sensitivity of SKA to dark matter induced radio emission, *JCAP* **09**, 025, arXiv:2105.00776 [astro-ph.HE].
- [59] G.-S. Wang, Z.-F. Chen, L. Zu, H. Gong, L. Feng, and Y.-Z. Fan, SKA sensitivity for possible radio emission from dark matter in Omega Centauri, (2023), arXiv:2303.14117 [astro-ph.HE].
- [60] A. Ghosh, A. Kar, and B. Mukhopadhyaya, Search for decaying heavy dark matter in an effective interaction framework: a comparison of  $\gamma$ -ray and radio observations, *JCAP* **09**, 003, arXiv:2001.08235 [hep-ph].
- [61] S. Colafrancesco, S. Profumo, and P. Ullio, Multi-frequency analysis of neutralino dark matter annihilations in the Coma cluster, *Astron. Astrophys.* **455**, 21 (2006), arXiv:astro-ph/0507575.
- [62] A. McDaniel, T. Jeltema, S. Profumo, and E. Storm, Multiwavelength Analysis of Dark Matter Annihilation and RX-DMFIT, *JCAP* **09**, 027, arXiv:1705.09384 [astro-ph.HE].
- [63] B. Dutta, A. Kar, and L. E. Strigari, Constraints on MeV dark matter and primordial black holes: Inverse Compton signals at the SKA, *JCAP* **03**, 011, arXiv:2010.05977 [astro-ph.HE].
- [64] L. Ferrario, D. de Martino, and B. Gaensicke, Magnetic White Dwarfs, *Space Sci. Rev.* **191**, 111 (2015), arXiv:1504.08072 [astro-ph.SR].
- [65] L. Ferrario, D. Wickramasinghe, and A. Kawka, Magnetic fields in isolated and interacting white dwarfs, *Advances in Space Research* **66**, 1025 (2020), arXiv:2001.10147 [astro-ph.SR].
- [66] S. Bagnulo and J. D. Landstreet, Multiple Channels for the Onset of Magnetism in Isolated White Dwarfs, *ApJL* **935**, L12 (2022), arXiv:2208.02655 [astro-ph.SR].
- [67] M. Boudaud, T. Lacroix, M. Stref, J. Lavalle, and P. Salati, In-depth analysis of the clustering of dark matter particles around primordial black holes. Part I. Density profiles, *JCAP* **08**, 053, arXiv:2106.07480 [astro-ph.CO].
- [68] P. Chanda, J. Scholtz, and J. Unwin, Improved Constraints on Dark Matter Annihilations Around Primordial Black Holes, (2022), arXiv:2209.07541 [hep-ph].

- [69] A. Loeb and M. Zaldarriaga, The Small-scale power spectrum of cold dark matter, *Phys. Rev. D* **71**, 103520 (2005), arXiv:astro-ph/0504112.
- [70] E. Bertschinger, The Effects of Cold Dark Matter Decoupling and Pair Annihilation on Cosmological Perturbations, *Phys. Rev. D* **74**, 063509 (2006), arXiv:astro-ph/0607319.
- [71] P. Gondolo, J. Hisano, and K. Kadota, The Effect of quark interactions on dark matter kinetic decoupling and the mass of the smallest dark halos, *Phys. Rev. D* **86**, 083523 (2012), arXiv:1205.1914 [hep-ph].
- [72] S. Profumo, K. Sigurdson, and M. Kamionkowski, What mass are the smallest protohalos?, *Phys. Rev. Lett.* **97**, 031301 (2006), arXiv:astro-ph/0603373.
- [73] P. Gondolo and K. Kadota, Late Kinetic Decoupling of Light Magnetic Dipole Dark Matter, *JCAP* **06**, 012, arXiv:1603.05783 [hep-ph].
- [74] A. M. Green, S. Hofmann, and D. J. Schwarz, The power spectrum of SUSY - CDM on sub-galactic scales, *Mon. Not. Roy. Astron. Soc.* **353**, L23 (2004), arXiv:astro-ph/0309621.
- [75] A. M. Green, S. Hofmann, and D. J. Schwarz, The First wimpy halos, *JCAP* **08**, 003, arXiv:astro-ph/0503387.
- [76] T. Bringmann and S. Hofmann, Thermal decoupling of WIMPs from first principles, *JCAP* **04**, 016, [Erratum: *JCAP* **03**, E02 (2016)], arXiv:hep-ph/0612238.
- [77] E. Vasiliev, Dark matter annihilation near a black hole: Plateau vs. weak cusp, *Phys. Rev. D* **76**, 103532 (2007), arXiv:0707.3334 [astro-ph].
- [78] L. Sadeghian, F. Ferrer, and C. M. Will, Dark matter distributions around massive black holes: A general relativistic analysis, *Phys. Rev. D* **88**, 063522 (2013), arXiv:1305.2619 [astro-ph.GA].
- [79] P. D. Serpico, V. Poulin, D. Inman, and K. Kohri, Cosmic microwave background bounds on primordial black holes including dark matter halo accretion, *Phys. Rev. Res.* **2**, 023204 (2020), arXiv:2002.10771 [astro-ph.CO].
- [80] P. Ullio, H. Zhao, and M. Kamionkowski, A Dark matter spike at the galactic center?, *Phys. Rev. D* **64**, 043504 (2001), arXiv:astro-ph/0101481.
- [81] S. L. Shapiro and D. C. Heggie, Effect of stars on the dark matter spike around a black hole: A tale of two treatments, *Phys. Rev. D* **106**, 043018 (2022), arXiv:2209.08105 [astro-ph.GA].
- [82] B. D. Fields, S. L. Shapiro, and J. Shelton, Galactic Center Gamma-Ray Excess from Dark Matter Annihilation: Is There A Black Hole Spike?, *Phys. Rev. Lett.* **113**, 151302 (2014), arXiv:1406.4856 [astro-ph.HE].
- [83] S. L. Shapiro and J. Shelton, Weak annihilation cusp inside the dark matter spike about a black hole, *Phys. Rev. D* **93**, 123510 (2016), arXiv:1606.01248 [astro-ph.HE].
- [84] G. B. Rybicki and A. P. Lightman, *Radiative processes in astrophysics* (1979).
- [85] G. Ghisellini, *Radiative Processes in High Energy Astrophysics*, Vol. 873 (2013).
- [86] T. R. Slatyer and C.-L. Wu, General Constraints on Dark Matter Decay from the Cosmic Microwave Background, *Phys. Rev. D* **95**, 023010 (2017), arXiv:1610.06933 [astro-ph.CO].
- [87] T. R. Slatyer, Indirect Detection of Dark Matter, arXiv:1710.05137 [hep-ph].
- [88] H. Liu, W. Qin, G. W. Ridgway, and T. R. Slatyer, Lyman- $\alpha$  constraints on cosmic heating from dark matter annihilation and decay, *Phys. Rev. D* **104**, 043514 (2021), arXiv:2008.01084 [astro-ph.CO].
- [89] M. Boudaud, J. Lavalle, and P. Salati, Novel cosmic-ray electron and positron constraints on MeV dark matter particles, *Phys. Rev. Lett.* **119**, 021103 (2017), arXiv:1612.07698 [astro-ph.HE].
- [90] M. Boudaud, Voyager probing Dark Matter, *PoS ICRC2019*, 512 (2021).
- [91] M. Boudaud and M. Cirelli, Voyager 1  $e^\pm$  Further Constrain Primordial Black Holes as Dark Matter, *Phys. Rev. Lett.* **122**, 041104 (2019), arXiv:1807.03075 [astro-ph.HE].
- [92] T. Enoto, S. Kisaka, and S. Shibata, Observational diversity of magnetized neutron stars, *Rept. Prog. Phys.* **82**, 106901 (2019).
- [93] T. Cohen, K. Murase, N. L. Rodd, B. R. Safdi, and Y. Soreq,  $\gamma$ -ray Constraints on Decaying Dark Matter and Implications for IceCube, *Phys. Rev. Lett.* **119**, 021102 (2017), arXiv:1612.05638 [hep-ph].
- [94] J. E. Koglin, F. E. Christensen, W. W. Craig, T. R. Decker, C. J. Hailey, F. A. Harrison, C. Hawthorn, C. P. Jensen, K. K. Madsen, M. Stern, G. Tajiri, and M. D. Taylor, NuSTAR hard x-ray optics, in *Optics for EUV, X-Ray, and Gamma-Ray Astronomy II*, Society of Photo-Optical Instrumentation Engineers (SPIE) Conference Series, Vol. 5900, edited by O. Citterio and S. L. O'Dell (2005) pp. 266–275.
- [95] P. Ferrando, SIMBOL-X, an X-ray telescope for the 0.5-70 keV range, in *SF2A-2002: Semaine de l'Astrophysique Francaise*, edited by F. Combes and D. Barret (2002) p. 271, arXiv:astro-ph/0210229 [astro-ph].
- [96] G. Lucchetta, M. Ackermann, D. Berge, and R. Bühler, Introducing the MeVCube concept: a CubeSat for MeV observations, *JCAP* **08** (08), 013, arXiv:2204.01325 [astro-ph.IM].
- [97] T. S. Yamamoto, R. Inui, Y. Tada, and S. Yokoyama, Prospects of detection of subsolar mass primordial black hole and white dwarf binary mergers, (2023), arXiv:2401.00044 [gr-qc].
- [98] G. Nelemans, L. R. Yungelson, and S. F. Portegies Zwart, The gravitational wave signal from the galactic disk population of binaries containing two compact objects, *Astron. Astrophys.* **375**, 890 (2001), arXiv:astro-ph/0105221.
- [99] K. Maguire, M. Eracleous, P. G. Jonker, M. MacLeod, and S. Rosswog, Tidal Disruptions of White Dwarfs: Theoretical Models and Observational Prospects, *Space Sci. Rev.* **216**, 39 (2020), arXiv:2004.00146 [astro-ph.HE].
- [100] H. Wang, A. P. Stephan, S. Naoz, B.-M. Hoang, and K. Breivik, Gravitational-wave Signatures from Compact Object Binaries in the Galactic Center, *Astrophys. J.* **917**, 76 (2021),

- arXiv:2010.15841 [astro-ph.HE].
- [101] Z. Xuan, S. Naoz, and X. Chen, Detecting accelerating eccentric binaries in the LISA band, *Phys. Rev. D* **107**, 043009 (2023), arXiv:2210.03129 [astro-ph.HE].
- [102] A. Sesana, A. Vecchio, M. Eracleous, and S. Sigurdsson, Observing white dwarfs orbiting massive black holes in the gravitational wave and electro-magnetic window, *MNRAS* **391**, 718 (2008), arXiv:0806.0624 [astro-ph].
- [103] P. A. Seoane *et al.* (LISA), Astrophysics with the Laser Interferometer Space Antenna, *Living Rev. Rel.* **26**, 2 (2023), arXiv:2203.06016 [gr-qc].
- [104] Y. Shao and X.-D. Li, Population Synthesis of Black Hole Binaries with Compact Star Companions, *Astrophys. J.* **920**, 81 (2021), arXiv:2107.03565 [astro-ph.HE].
- [105] K. Qin, L. Jiang, and W.-C. Chen, Black Hole Ultra-compact X-Ray Binaries: Galactic Low-frequency Gravitational Wave Sources, *Astrophys. J.* **944**, 83 (2023), arXiv:2301.06243 [astro-ph.HE].
- [106] S. Rosswog, E. Ramirez-Ruiz, and W. R. Hix, Tidal Disruption and Ignition of White Dwarfs by Moderately Massive Black Holes, *Astrophys. J.* (2009).
- [107] C.-Q. Ye, J.-H. Chen, J.-d. Zhang, H.-M. Fan, and Y.-M. Hu, Observing white dwarf tidal stripping with TianQin gravitational wave observatory, *MNRAS* 10.1093/mnras/stad3296 (2023), arXiv:2307.08231 [astro-ph.HE].
- [108] C. S. Ye, G. Fragione, and R. Perna, On the Tidal Capture of White Dwarfs by Intermediate-mass Black Holes in Dense Stellar Environments, *Astrophys. J.* **953**, 141 (2023), arXiv:2303.07375 [astro-ph.HE].

